Letters

DC/DC Converter With High Current Capability for All DC Renewable System

Yingzong Jiao, *Member, IEEE*, Binbin Li, *Senior Member, IEEE*, Lianzheng Ding, Zhiwen Suo, and Dianguo Xu, *Fellow, IEEE*

***Abstract*—High current, efficiency, and compactness are the key challenges of dc/dc converters for all dc renewable system. In this letter, a dc/dc converters is proposed to address these challenges. The proposed converter incorporates three key innovations: parallel operation, direct transmission of partial power, and non-ac energy balancing. Through parallel operation, the converter facilitates the sharing of current across multiple strings of submodules, resulting in high current capability. Furthermore, the integration of direct transmission of partial power and non-ac energy balancing minimize installations of insulated gate bipolar transistors (IGBTs) and capacitors, contributes to enhanced efficiency and compactness. The effectiveness and validity of the proposed converter are demonstrated through simulation and experimental results.**

***Index Terms*—DC/DC converter, direct transmission of partial power, high current, non-ac energy balancing, parallel operation.**

I. Introduction

THE field of renewable power generation is undergoing rapid development [1]. As the capacity of renewable energy plants continues to rise, the adoption of all dc collection and transmission system emerges as a promising solution for future large-scale renewable plants, as illustrated in Fig. 1. The all dc system has the potential to reduce cable losses in the renewable power collection and enhance system reliability [2]. The high-power dc/dc converters, responsible for stepping up the voltage from medium voltage direct current (MVDC) to high voltage direct current (HVDC), stands out as the most critical equipment in the all dc system [3]. It must possess with high power rating, efficiency, low cost, and small footprint, particularly in offshore applications. Notably, a significant challenge arises from the current stress at MVDC side. The limited current capacity of commercial insulated gate bipolar transistor (IGBT), maxing at 3000 A, restricts the power rating of the dc/dc converter, making it unable to meet the HVDC transmission power levels.

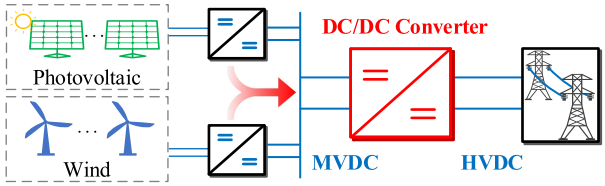

Fig. 1. Configuration of the all DC renewable energy system.

Several well-researched high-power dc/dc topologies exist in the literatures. The front-to-front modular multilevel converters (FTF-MMC)-based dc/dc converter is most straightforward, which integrates two MMC with a transformer on the ac side [4]. However, the FTF-MMC has notable drawbacks of high component count, large volume, and increased loss. This is attributed to the three full-power conversion stages: dc/ac, magnetic ac/ac, and dc/ac. An alternative configuration, dc autotransformer [5], employs two MMCs connected in series on the dc ports while interconnected on the ac side through a transformer. Despite reducing power rating of the ac transformer, it faces challenge of high dc-offset voltage, leading to increasing volume and insulation effort. In [6], cascaded submodules (SMs) are cross-connected between the upper and lower MMCs to replace the ac transformer, but this is at the expense of higher installed capacity of semiconductor components. The direct current modular multilevel converter (DCMMC) converter, as discussed in [7], uses only one MMC to generate the dc voltage directly. Nevertheless, it requires high inner ac currents and bulky filters to achieve the energy balance of SMs in the DCMMC. The power loss and footprint are significant.

To enhance power conversion efficiency, a hybrid modular dc/dc converter has been introduced in [8] and [9], combining the merits of low cost, low conduction loss, and high robustness of thyristors or diodes, with the high controllability of the cascaded SMs. However, each cascaded SM string still needs to sustain the entire MVDC current and the HVDC voltage. This necessitates a high installation of semiconductors and substantial energy storage in the SM capacitors. Most importantly, it constrains the converter power rating due to the limited MVDC current imposed by the available IGBT current rating.

In order to overcome the current technical limitations, this letter proposes a novel dc/dc converter designed for all dc

Manuscript received 2 January 2024; revised 13 February 2024; accepted 7 March 2024. Date of publication 14 March 2024; date of current version 4 September 2024. This work was supported by National Key Research and Development Program of China under Grant 2023YFB2407202. *(Corresponding author: Binbin Li.)*

Yingzong Jiao, Binbin Li, Lianzheng Ding, and Dianguo Xu are with the School of Electrical Engineering, Harbin Institute of Technology, Harbin 150001, China (e-mail: jiaoyingzong@hit.edu.cn; libinbin@hit.edu.cn; dinglz@stu.hit.edu.cn; xudiang@hit.edu.cn).

Zhiwen Suo is with the State Grid Economic and Technological Research Institute Company, Ltd., Beijing 102209, China (e-mail: suozhiwen@chinasperi.sgcc.com.cn).

Color versions of one or more figures in this article are available at https://doi.org/10.1109/TPEL.2024.3377290.

Digital Object Identifier 10.1109/TPEL.2024.3377290

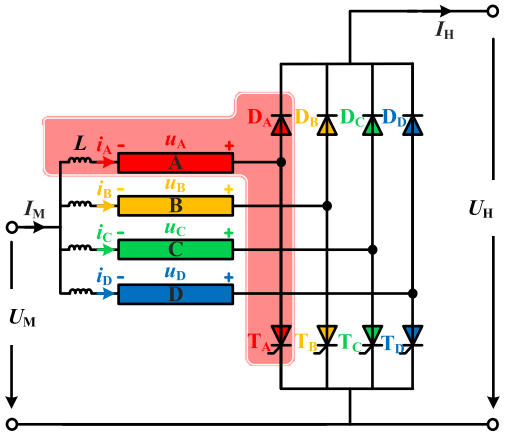

Fig. 2. Circuit configuration of the proposed DC/DC converter.

renewable system. The proposed converter incorporates three key innovations: parallel operation, direct transmission of partial power, and non-ac energy balancing. Through parallel operation, the converter facilitates the sharing of MV current across multiple strings of SMs, resulting in high current capability. Furthermore, the integration of direct transmission of partial power and non-ac energy balancing for SMs reduces the requisite number of SMs. This reduction, coupled with minimized installations of IGBTs and capacitors, contributes to enhanced efficiency and compactness. Hence, high current, efficiency, and compactness are the main contributions of proposed converter.

II. Topology and Operating Principle

A. Topology

Fig. 2 depicts the circuit configuration of the proposed dc/dc converter. It consists of four parallel units j (j = A, B, C, and D), where each unit has one SMs string j, an upper diodes valve D_j, a bottom thyristors valve T_j, and one induct L. Each string is composed of N full-bridge SMs connected in series. By employing full-bridge SMs, the dc converter can effectively mitigate and isolate the impact of faults on dc system. The terms U_M and I_M are the voltage and current of the MVDC side, U_H and I_H are the voltage and current of the HVDC side.

B. Operation Principle

The basic operational principles of the proposed dc/dc converter are as follows.

1) *Parallel Operation:* At any moment, there are at least three units to distribute the current of the MVDC side. Furthermore, the current capacity can be expanded by adding more units. Assuming there are n units, and the maximum current of commercial IGBTs is 3000 A, the total maximum current of the MVDC side can be (n-1) × 3000 A. For instance, considering the configuration depicted in Fig. 2, the maximum current is up to 9000 A.
2) *Direct Transmission of Partial Power:* At least one unit serves as a connection between MVDC and HVDC, facilitating the direct transmission of power from MVDC to HVDC. This unit offers only the voltage difference between MVDC and HVDC, not the entire voltage of HVDC. Consequently, the need for installing SMs can be minimized. In addition, the partial power (1/r of rated power, where r is the ratio of U_H/U_M) is directly transmitted. As a result, the requirement for energy storage in SMs can also be reduced.
3) *Non-AC Energy Balancing:* The SMs in the proposed dc/dc converter achieve energy balance through interleaved connections with both the MVDC and HVDC sides. When connected to the MVDC side, the SMs absorb energy, and when connected to the HVDC side, they release energy. The diode and thyristor valves provide current paths when the SMs are connected to HVDC and MVDC, respectively, and also bear the voltage stress. Simultaneously, the SMs generate appropriate voltages to regulate the unit currents and ensure reliable thyristor turn-OFF. This approach effectively mitigates inner ac voltage and current in DCMMC [7], resulting in high-efficiency energy balancing and minimizing the required installation of SMs.

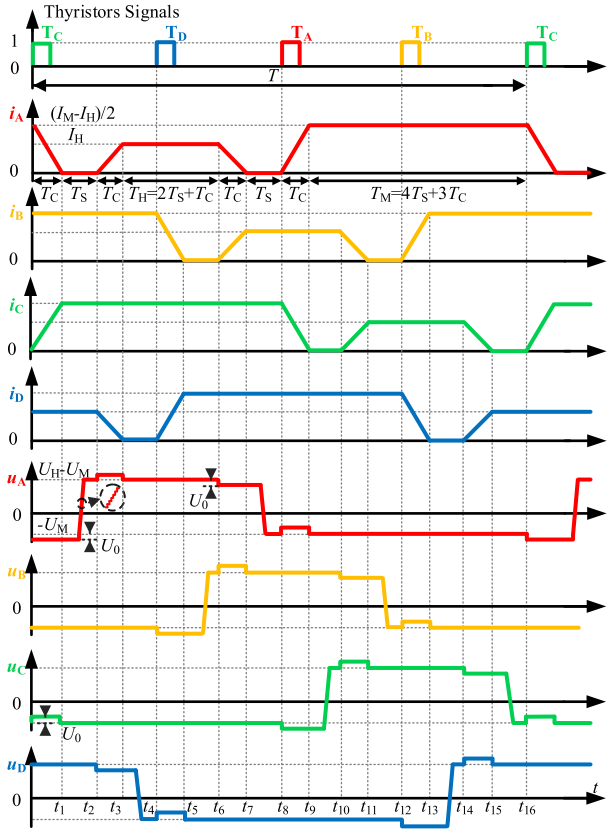

Fig. 3. Sketched operating waveforms of the proposed DC/DC converter.

The detailed operational waveforms of the proposed dc/dc converter are depicted in Fig. 3. All unit currents exhibit identical but interleaved trapezoidal waveforms, with the currents of four units interleaving with one-fourth of a cycle. Using the time interval $[t_5, t_9]$ as the example, the operating analysis is presented in the Fig. 4 and Table I.

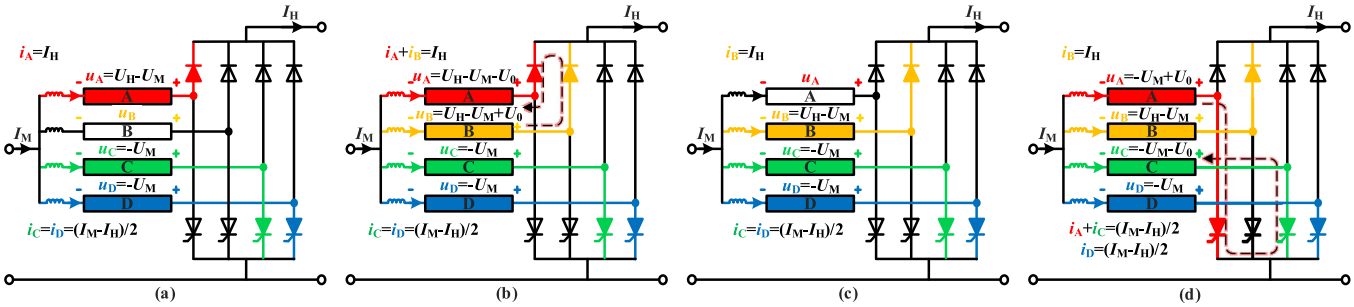

Fig. 4. Operation analysis of proposed DC/DC converter during different time intervals. (a) $[t_5, t_6]$. (b) $[t_6, t_7]$. (c) $[t_7, t_8]$. (d) $[t_8, t_9]$.

TABLE I
VOLTAGES AND CURRENTS DURING NON-AC ENERGY BALANCE OF UNIT A

	u_A/i_A	u_B/i_B	u_C/i_C	u_D/i_D
$[t_5, t_6]$	U_H-U_M I_H	-U_M→U_H-U_M 0	-U_M (I_L-I_H)/2	-U_M (I_L-I_H)/2
$[t_6, t_7]$	U_H-U_M-U_0 I_H→0	U_H-U_M+U_0 0→I_H	-U_M (I_L-I_H)/2	-U_M (I_L-I_H)/2
$[t_7, t_8]$	U_H-U_M→-U_M 0	U_H-U_M I_H	-U_M (I_L-I_H)/2	-U_M (I_L-I_H)/2
$[t_8, t_9]$	-U_M+U_0 0→(I_L-I_H)/2	U_H-U_M I_H	-U_M-U_0 0→(I_L-I_H)/2	-U_M (I_L-I_H)/2

TABLE II
SIMULATION AND EXPERIMENTAL PARAMETERS

Parameters	Simulations	Experimental
Power rating	900 MW	1.2 kW
HVDC voltage U_H	300 kV	300 V
MVDC voltage U_M	100 kV	100 V
Capacitor voltage (U_C)	2500 V	90 V
Number of SMs of per phase	100	3
SM capacitance (C)	10 mF	6 mF
String inductance (L)	8 mH	4 mH
Carrier frequency	300 Hz	3 kHz
Commutation time (T_C)	500 μs	1 ms
Steady-state time (T_S)	750 μs	500 μs

It can be seen that, there are at least three units to distribute the MVDC current (during $[t_5, t_6]$, units A, C, and D share the current) in each moment, and there is also at least one unit which inserts between MVDC and HVDC and transmits power directly (e.g., at $[t_5, t_6]$, unit A directly transmits power). In this way, as depicted in Fig. 4(a), parallel operation and direct power transmission are realized in the proposed dc/dc converter.

As for the non-ac energy balancing, the SMs of each unit generate appropriate voltages to regulate the currents and realize current commutation. The current paths of the non-ac energy balancing of unit A during $[t_6, t_7]$ are given in the Fig. 4(b)–(d). During $[t_6, t_7]$, unit A generates U_H-U_M-U_0, and unit B generates U_H-U_M-U_0, resulting in the current commutation between unit A and B, where U_0 is the driving voltage ($U_0 = (t_7\text{-}t_6) \times I_H/L$). The driving voltage also turn OFF the diode and thyristor valves reliably. After the currents of units are 0, the voltages of units are controlled in staircase waveform during the rising and falling transitions to limit du/dt, e.g., at $[t_7, t_8]$, unit A voltage is controlled from U_H-U_M-U_0 to -U_M in staircase. With the operation principle, non-ac energy balance is realized, resulting in improving the efficiency and reducing SM installation number and capacitors.

Based on the aforementioned analysis, the power transfer from MVDC to HVDC and the energy balance for each unit are achieved. The capacitors of the SMs should be designed to tolerate the energy fluctuations of each unit

$$C = \frac{\Delta E_{\max}}{2N\varepsilon U_C^2} = \frac{\left(1-\frac{1}{r}\right)PT}{8N\varepsilon U_C^2} \tag{1}$$

where $\Delta E_{\max}$ is the maximum energy fluctuations in one cycle, which is equal to the partial power processed by the units, $r = U_H/U_M$ is the voltage ratio between MVDC and HVDC, P is the rated power, T is the period time, ε is the relative voltage ripple, and U_C is the rated capacitor voltage.

III. EVALUATION AND COMPARISON

A. Simulation and Experimental Results

To evaluate the validity of the proposed dc/dc converter, simulation was carried out with a case of 100 /300 kV, 9000 A at MVDC side. The detailed parameters are listed in Table II. The simulation results are illustrated in Fig. 5. The U_H and U_M are the continuous dc voltages, and I_H and I_M are continuous 3000 and 9000 A, respectively. The currents of four units are controlled as identical but interleaved with 1/4 period, (I_M-I_H)/2 and I_H are equal to 3000 A. In the context of parallel operation, u_A is 200 kV (U_H-U_M) when the unit A connects between MVDC and HVDC, current i_A constitutes I_H, and unit A directly transmits 1/3 partial power. Conversely, u_A is −100 kV (U_M) when parallel with MVDC and i_A constitutes (I_M-I_H)/2. Although the current of one unit is a trapezoidal waveform, with parallel operation, four units together constitute constant current in both MVDC and HVDC. The driving voltage occurs during current commutation, and the capacitor voltage is kept well balanced.

Furthermore, a down-scaled the proposed dc/dc prototype at 100/300 V, has been built and tested to validate the operational behaviors. The prototype photograph and results are depicted in the Figs. 6 and 7. The four units together constitute constant currents in both MVDC and HVDC with interleaved waveforms, demonstrating consistency with the simulation. It is worth noting that due to the limited number of SMs, the generated voltage waveform exhibits fewer voltage steps and more fluctuations in currents compared with the simulation results.

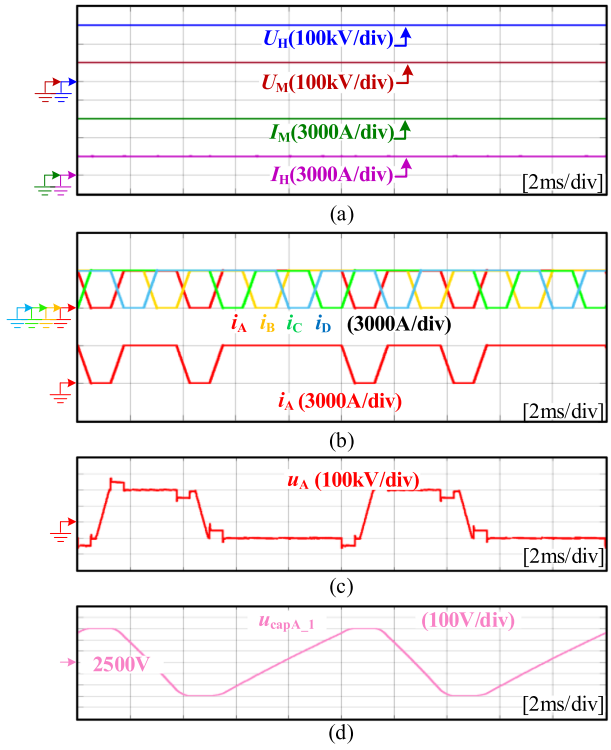

Fig. 5. Simulation results of the proposed DC/DC converter. (a) Voltages and currents. (b) Phase currents and i_A. (c) Output voltage u_A. (d) Summation of SM capacitor voltage.

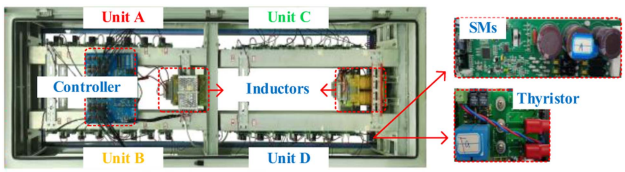

Fig. 6. Configuration and photograph of the scaled-down DC/DC converter.

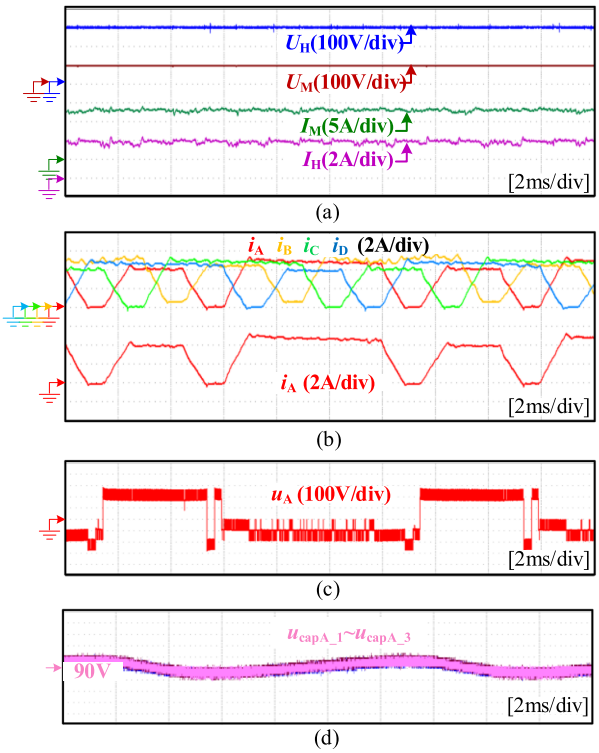

Fig. 7. Experimental results of the proposed DC/DC converter. (a) Voltages and currents. (b) Phase currents and i_A. (c) Output voltage u_A. (d) SM capacitor voltage.

TABLE III
COMPARISON WITH EXISTING DC/DC CONVERTERS

Parameters	Proposed	[7]	Unidirectional [9]
Number of SMs	**400**	**1800**	**1143**
Number of IGBTs	1600	5760	2286
Number of Diodes	260	/	774
Number of Thyristors	260	/	/
Total loss (MW)	**11.01**	**32.30**	**11.37**
Conduction loss of IGBTs	7.67	23.05	5.64
Switch loss of IGBTs	2.63	9.25	5.22
Conduction loss of Thyristors	0.51	/	/
Conduction loss of Diodes	0.20	/	0.51
Energy Storage (kJ/MW)	**16.67**	**56.4**	**25**

The important comparison results are represented in bold entities.

B. Comparison With DCMMC [7] and Hybrid Modular [9]

In the comparative analysis of the proposed dc/dc converter with the DCMMC [7] and hybrid modular dc/dc converter [9], the simulation parameters outlined in Table II serve as the basis for the case study, and the corresponding results are presented in Table III. To facilitate a fair comparison, the configuration of reference [9] has been adapted to a unidirectional setup, where diodes have been substituted for thyristors. Utilizing the 5SNA 3000K452300 for IGBT, the 5SDD 75Y8500 for diodes, and the 5STP 45Y8500 for thyristors, remains consistent across all configurations. A derating factor of 0.55 is applied to diodes and thyristors for series connection.

It is noteworthy that, owing to the direct transmission of partial power and non-ac energy balancing, the proposed dc/dc converter presents significantly reduced number of SMs, accounting for only 22% compared with [7] and 35% to [9]. Moreover, with non-ac energy balancing, the proposed dc/dc converter also exhibits a significant reduction in total power loss and energy storage demand, accounting for only 34.08% in total power loss and 29.6% in energy storage compared with [7]. Furthermore, there is a reduction of 1/3 in demand for energy storage in capacitors compared with [9], attributed to the direct transmission of 1/3 of the power. These characteristics collectively contribute to the proposed dc/dc converter presenting a highly efficient and compact solution.

C. Generalization of Proposed Converter With More Units

The benefits of the proposed dc/dc converter have been evaluated by experimental tests and performance comparison. The high current capability of the system is due to the parallel operation of units, allowing for convenient expansion of current capacity by incorporating additional units. In this configuration,

the maximum current on the MVDC side can reach up to (n-1) $\times$ 3000 A when the units increases to n.

However, the overall period with n units can be expressed as $T = 2n \times (T_S + T_C)$, indicating a direct relationship between the number of units and the operating period. As the operating period increases linearly, so does the energy storage requirement, according to (1). Therefore, it is crucial to consider the impact on the operating period and capacitance energy storage to ensure it remains within acceptable limits.

IV. Conclusion

This letter introduces a novel high current capability dc/dc converter for all dc renewable system. Employing parallel operation, direct transmission of partial-power and non-ac energy balance, the characteristics of high current, efficiency, and compactness can be reached. The effectiveness is validated through simulations and downscaled tests, and the comparison highlights the contributions of proposed converter. The discussion on the generalization of more units also illustrates the expanding and limit of parallel operation.

References

[1] P. Bresesti, W. L. Kling, R. L. Hendriks, and R. Vailati, "HVDC connection of offshore wind farms to the transmission system," *IEEE Trans. Energy Convers.*, vol. 22, no. 1, pp. 37–43, Mar. 2007.

[2] K. Musasa, N. I. Nwulu, M. N. Gitau, and R. C. Bansal, "Review on DC collection grids for offshore wind farms with high-voltage DC transmission system," *Inst. Eng. Technol. Power Electron.*, vol. 10, no. 15, pp. 2104–2115, 2017.

[3] Z. Li, Q. Song, F. An, B. Zhao, Z. Yu, and R. Zeng, "Review on DC transmission systems for integrating large-scale offshore wind farms," *Energy Convers. Econ.*, vol. 2, no. 1, pp. 1–14, 2021.

[4] T. Lüth, M. M. C. Merlin, T. C. Green, F. Hassan, and C. D. Barker, "High-frequency operation of a DC/AC/DC system for HVDC applications," *IEEE Trans. Power Electron.*, vol. 29, no. 8, pp. 4107–4115, Aug. 2014.

[5] W. Lin, "DC–DC autotransformer with bidirectional DC fault isolating capability," *IEEE Trans. Power Electron.*, vol. 31, no. 8, pp. 5400–5410, Aug. 2016.

[6] S. Du, B. Wu, and N. R. Zargari, "A transformerless high-voltage DC–DC converter for DC grid interconnection," *IEEE Trans. Power Del.*, vol. 33, no. 1, pp. 282–290, Feb. 2018.

[7] F. Zhang, W. Li, and G. Joós, "A transformerless hybrid modular multilevel DC–DC converter with DC fault ride-through capability," *IEEE Trans. Ind. Electron.*, vol. 66, no. 3, pp. 2217–2226, Mar. 2019.

[8] B. Li, X. Zhao, S. Zhang, Q. Fu, S. Wang, and D. Xu, "A hybrid modular DC/DC converter for HVDC applications," *IEEE Trans. Power Electron.*, vol. 35, no. 4, pp. 3377–3389, Apr. 2020.

[9] B. Li, B. Zhang, Y. Zhang, L. Li, and D. Xu, "Design and implementation of a high-power DC/DC converter for HVDC interconnections with wide DC voltage range and fault-blocking capability," *IEEE J. Emerg. Sel. Topics Power Electron.*, vol. 10, no. 1, pp. 785–799, Feb. 2022.